Design and Application of New Impeller-Type Wax-Proof Device Based on Speed-Increasing Wax-Proof Mechanism

Zi-ming Feng[1*], Yi Sun[1], Xiaolei Liu[2*], Wei Cui[1], Weibo Duan[1]
[1] School of Mechanical Science and Engineering, Northeast Petroleum University, Daqing, China.
[2]School of Engineering, University of Glasgow, G12 8QQ, Glasgow, UK

Abstract: Wax deposition in oil wells seriously affects hydrocarbon production and causes inevitable economic losses. Especially in rodless pumping wells, due to the lack of the stirring effect of the sucker rod, the waxing of the tubing is more serious. According to the correlation law between flow velocity and wax deposition, a speed-increasing impeller wax prevention device was designed. Based on fluid dynamics, the influence of impeller geometry and equipment process parameters on wax deposition was studied, and the optimization design of the device was proposed. After that, CFD simulations were used to determine the structure parameters of the wax-proof device. The diameters of the impeller hub and rim are 34 mm and 60 mm, respectively; the axial length of the impeller is 42 mm; the number of blades is five; the rotation speed is 600 r/min. The inlet and outlet angle of the blade was designed based on the increasing ability of the impeller's speed. The head of the impeller is used as the basis for determining the distance of the paraffin preventer. Starting from the position prone to the wax deposition, place multiple wax-proof impellers in series in the wellbore. Comparing with traditional wax prevention methods, our experiments showed that this wax-proof device has a good function in wax prevention and improves the economic benefit of high waxy wells. This paper provides a new choice for wax-proof device.

Keywords: Waxing; Diversion Impeller; Speed-increasing Wax Prevention; Spiral Flow

1 Introduction

In the process of oil extraction, with the decrease of temperature, pressure, and flow rate of the well fluids, wax molecules will precipitate out of crude oil and gradually move to the pipe wall with low temperature, forming a concentration gradient of oil wall wax molecules. Those molecules will eventually gather into the core, then form deposited wax. Oil well waxing can cause many hazards, such as clogging of tubing, reducing production, and more seriously damaging oil extraction equipment. For instance, in the Lasmo oil field of the UK, the wax deposition issues directly caused the field to be abandoned, where the economic loss was over100 million US dollars [1]. For oilfields worldwide, waxing has become one of the most challenging difficulties, especially for rodless pumping wells. These difficulties include low flow rates of well fluid, lacking reciprocating movement of the sucker rod in the well, and less turbulent well fluid flows [2].

In response to this issue, researchers have proposed a variety of wax removal techniques and equipment, including thermal wax removal and the use of mechanical devices, chemical agents, and microorganisms [3, 4].

The most common application of thermal cleaning and anti-wax technology is to inject heat carriers, such as hot oil or hot water, into the well to increase the temperature of the tubing and crude oil for preventing the occurrence of wax deposition. It has the advantages of simple operations, thorough wax cleaning, and low costs [5]. However, it may cause formation pollution and even oil production reduction [6].

Mechanical wax removing uses a scraper device to graze the wax on the sucker rod and the pipe wall. It is widely used and has the advantages of easy operations and low costs. The

disadvantage is that it is impossible to completely remove the deposited wax in the tubing because it is easy to damage the equipment and to cause wax blocking, etc. [7].

The chemical dewaxing technology mainly uses paraffin inhibitors or chemical solvents to achieve the purpose of dewaxing. To some degree, paraffin inhibitors can reduce wax deposits, improving the fluidity of crude oil, and increasing the solubility of paraffin wax in the mixture fluid [8, 9]. If the correct method is used, its validity period can be exceeded for 6 months [10]. However, if the inhibitor is used for a long time, it will pollute the formation and make the oil well dependent. With the increase of use time, the dosage of drugs will gradually rise, and the cycle of drugs will gradually shorten [11].

Microbial dewaxing is functional through the cultivation and screening of strains that are suitable for specific oils, injecting them into oil wells to produce a similar effect as chemical agents [1]. Its advantage is that it has a significant effect and does not cause considerable changes in oil quality. However, the application environment of microbial dewaxing is harsh, and it is only suitable for oil wells with a bottom hole temperature of less than 210 ° F. At the same time, some aerobic bacteria may cause corrosion [12].

Although the above-mentioned wax-removing and anti-waxing technologies have many applications, they all have unavoidable shortcomings. Therefore, it is necessary to find a novel method for efficiently solving the problem of wax deposition. Factors affecting the wax deposition, such as flow rates, crude oil properties, temperature, mechanical impurities & water, flow rate, and tube wall characteristics, etc., are often overlooked. The flow rate of the well fluid can largely affect the wax deposition rate and the amount of wax deposition.

Jessen et al. (1958) [13] proposed that increasing the shear rate will have different effects on wax deposition under different flow conditions. When the flow state is laminar, the increase of the shear rate will cause the mass of wax deposits on the pipe wall. Besides, the opposite is true for turbulent flow. Hartely et al. (1989) [14] considered that under turbulent flow, increasing the flow rate of well fluid will decrease the amount of wax deposition. Hsu et al. (1996) [15] studied the relationship between flow velocity and wax deposition under a single-phase flow condition through experiments. The results showed that when the flow velocity reaches about 4.24 m/s, the wax deposition rate will become very low. Nazar et al. (2005) [16] pointed out that the increase of flow rate can lead to an increase in the amount of wax deposition until the flow rate increases to a certain value, that is, the critical flow rate. When the flow rate continues to increase, it will cause a decrease in the quality of the sediment. Karami et al. (2011) [17] suggested that the ratio of the wax deposition amount and the shear stress of the pipe wall to the temperature difference is inversely proportional between the crude oil and the pipe wall. Rittirong (2014) [16] pointed out through experiments that although the increase in the gas flow rate will increase the thickness of the wax deposition when the gas and liquid velocities are increased at the same time, the wax layer thickness and deposition rate will decrease at the same time. Theyab et al. (2016) [19] conducted an experimental study on the effect of spiral flow on the wax deposition volume. The results showed that spiral flow can effectively delay the occurrence of wax deposition, and the inhibition efficiency of wax deposition at the same oil temperature is higher than chemical inhibitors. Albagli et al. (2017) [20] verified through experiments that if the Reynolds number of the fluid is increased, the amount of wax deposition will decrease. Alnaimat et al. (2020) [21] proposed various wax prediction methods for estimating wax deposition.

Based on the disclosure of the correlation between the fluid flow rate and the wax deposition

in the above-mentioned literature, a new speed-increasing impeller type wax prevention device is proposed and designed in this paper. This device can reduce wax deposition by increasing the flow rate of the produced fluid. Based on CFD results, the CFX software was used to analyze the hydraulic performance and optimize the structure of the wax-proof device. The experimental results showed that, when the device is used in oil production, the daily output within 30 days rises significantly. The electric pump current slowly increases, and the working level decreases by a small amount, indicating that the device has a great performance. The wax-proof improves the efficiency of oil recovery and reduces the period of well washing and pump inspection.

2 Structure of Impeller-type speed-increasing anti-wax device and theoretical basis

2.1 The structure of Impeller-type speed-increasing anti-wax device

In this study, an impeller type wax prevention device was invented based on the principle of speed-increasing wax prevention, and its structure is shown in **Fig. 1**. The equipment uses impellers (15) as a speed-increasing component, where a plurality of impellers (15) are connected in series by a rotating shaft, driven by a belt (3), and a three-phase asynchronous motor (1) at the wellhead. When the device is in operation, the impellers (15) can directly act on the well fluid, generating spiral flow while increasing the fluid flow rate to achieve the purpose of preventing wax. Since the setting of the rotating shaft directly leads to an increase in the area of wax deposition in the oil well, a hollow rod (14) is used to connect the impellers (15), and a check valve (18) is provided at the bottom end. The hot washing process can be directly performed if necessary. A shaft seal is provided at the center cross (12), and the sealing is realized through a packing seal, which is used to seal the leakage channel between the hollow rod (14) and the wall surface.

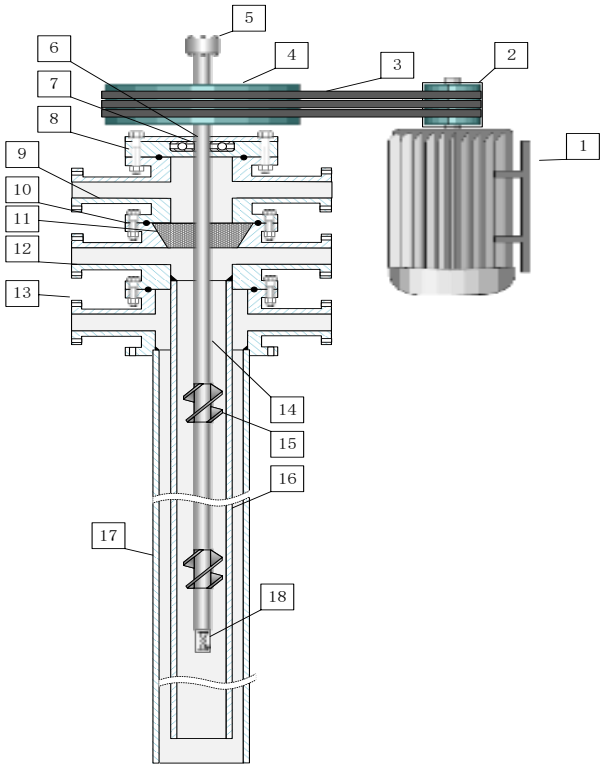

1-Three-phase Asynchronous Motor；2-Small pulley；3-Belt；4-Large pulley；
5-Flange joint；6-Bearing cap；7-Bearing；8-Bearing Seat；9-Upper Stone；

10-Fastening Bolt；11-Shaft Seal；12-Central Stone；13-Lower Stone；
14-Hollow Rod；15-Impellers；16-Tubing；17-Casing；18-Check Valve

Fig.1 Impeller Diversion Type Anti-Wax Device Structure Diagram

The impellers are the core of the wax prevention device, and their structure plays a vital role in wax prevention. In this paper, based on CFD, the influence of impeller structure parameters and device process parameters on speed increase and wax resistance will be studied. Then, the impeller diameter, blade inlet, and outlet angle, impeller length, blade number, impeller speed, impeller position, and spacing, etc. will be determined.

2.2 The major technical parameters

The major technical parameters of the impeller type speed-increasing anti-wax device are shown in **Table 1**.

Table 1 The Major Technical Parameters of Impeller Type Speed Increasing Anti-Wax Device

Parameter	Value
Oil Well Type	Rodless Wells
Oil Production	＜1576 t/day

2.3 Theoretical basis and Boundary conditions

In this simulation work, the flow medium was a single-phase, isothermal, and incompressible flow of oil inside the impeller passage.

The internal flow of oil well follows the rules of mass conservation equation, momentum conservation equation, and energy conservation equation.

Mass conservation equation for the flow model can be stated as follows [22]:

$$\frac{\partial \rho}{\partial t}+\frac{\partial(\rho u)}{\partial x}+\frac{\partial(\rho v)}{\partial y}+\frac{\partial(\rho w)}{\partial z}=0 \tag{1}$$

Where

ρ — density, kg/m³;

T — time, s.

u, v, and w — velocity vector components in the x, y, and z-direction, respectively.

The momentum conversation equation for the internal flow model of the oil well is as follows:

Regarding the rule, the momentum conversation equation in the x, y, and z-directions can be expressed as follows:

$$\begin{cases} \dfrac{\partial(\rho u)}{\partial t}+div(\rho u\vec{u})=-\dfrac{\partial p}{\partial x}+\dfrac{\partial \tau_{xx}}{\partial x}+\dfrac{\partial \tau_{yx}}{\partial y}+\dfrac{\partial \tau_{zx}}{\partial z}+F_x \\ \dfrac{\partial(\rho v)}{\partial t}+div(\rho v\vec{u})=-\dfrac{\partial p}{\partial y}+\dfrac{\partial \tau_{xy}}{\partial x}+\dfrac{\partial \tau_{yy}}{\partial y}+\dfrac{\partial \tau_{zy}}{\partial z}+F_y \\ \dfrac{\partial(\rho w)}{\partial t}+div(\rho w\vec{u})=-\dfrac{\partial p}{\partial z}+\dfrac{\partial \tau_{xz}}{\partial x}+\dfrac{\partial \tau_{yz}}{\partial y}+\dfrac{\partial \tau_{zz}}{\partial z}+F_z \end{cases} \tag{2}$$

Where

p —pressure on the elemental flow volume;

τ_{xx}, τ_{yx}, τ_{zx} — vector components of viscous stress;

F_x, F_y, F_z — body force on the elemental volume.

Reasonable boundary conditions can benefit the actual use of numerical simulations to analyze and solve issues related to flow. Also, it will have a huge impact on the convergence and the accuracy of the model. For the inlet, we defined that the flow rate of the well fluid is always at a level that delays the occurrence of wax deposition, so the inlet boundary is set to Normal speed 4.24 m/s. For

the outlet, it is assumed that the outlet is the wellhead, so the average static pressure is set to the average static pressure of 1 atm. The settings of other boundary conditions are described as follows:

The Wall surface is no-slip. The domain used for simulation in this article includes two parts: due to the impeller needs to be rotated, the domain where the impeller exists is defined as the rotating domain. Correspondingly, the rest is used as the stationary domain. Besides, the interface is set to General Connection. Due to the impeller domain similar to the domain in the axial flow pump, the interface between the rotating domain and the stationary domain was selected as Stage and Stage Average Velocity, respectively, for coupling.

The convergence accuracy of the simulation was set to 10^{-4}, and the maximum number of iteration steps was set to 2000.

2.4 Modeling and meshing

2.4.1 Geometric model

The establishment of the simulating model was completed by CFTurbo and SolidWorks. **Table 2** shows the initial parameters used in the modeling effort.

Table. 2 Initial Parameters of The Simulating Model

Hollow Rod Diameter / Impeller Hub Diameter	Impeller Rim Diameter	Blade Angle（5 spans）		Impeller Length	The Number of blades	Blade Thickness	Tubing Inner Diameter
		β_1	β_2				
36mm	68mm	45.6°	60.0°	30mm	6	1mm	76mm
		38.3°	50.4°				
		31.8°	40.8°				
		23.7°	31.2°				
		16.4°	21.6°				

Fig. 2 is the model diagrams based on the above parameters.

Fig.2 The Impeller and Pipeline Model Diagrams

2.4.2 Meshing and grid independence verification

2.4.2.1 Meshing

The meshing work was done by using ICEM CFD. The structure of the impeller contains a large area of curvature change and a torsional surface, and the pipe is a more regular ring structure. To better reflect the geometric characteristics of the device and reduce the number of grids, a hybrid of structural grids and unstructured grids is used in grid division. **Fig. 3** shows the drawn watershed grids.

（a）Inlet and Outlet Grids (Structural Grids)

（b）Impeller Grids (Unstructured Grids)

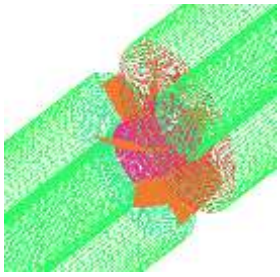

（c）Grids at Interface

Fig.3 Grids for Each Domain

After checking the grids, it was found that the quality of all grids was greater than 0.3 while the minimum angle was greater than 18°. Besides, the twist was less than 9°, which met the minimum requirements for ANSYS CFX.

2.4.2.2 Grid independence verification

In the numerical simulation, the number of mesh elements will have a significant impact on the simulation results and efficiency, so it is necessary to verify the mesh elements' independence. For the models involved in this paper, a total of 7 different meshes with different densities are divided. The numbers of mesh elements are 429190, 963329, 1298205, 1474336, 1880985, 2308807, and 2623251, respectively. The above seven models with different mesh densities were tested to perform flow simulation under the same working conditions to check the head and the efficiency. **Fig. 4** shows the simulation results.

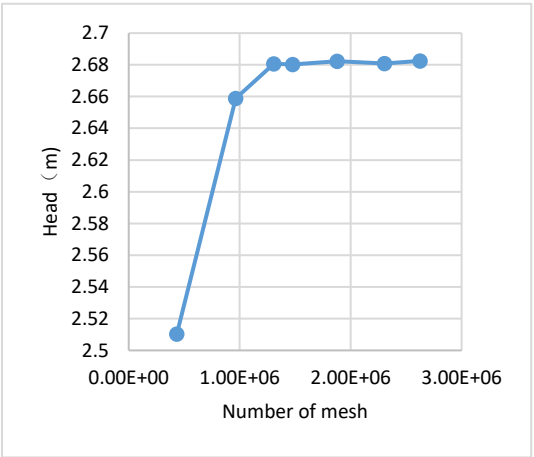

（a）Number of Mesh Elements-Head Curve

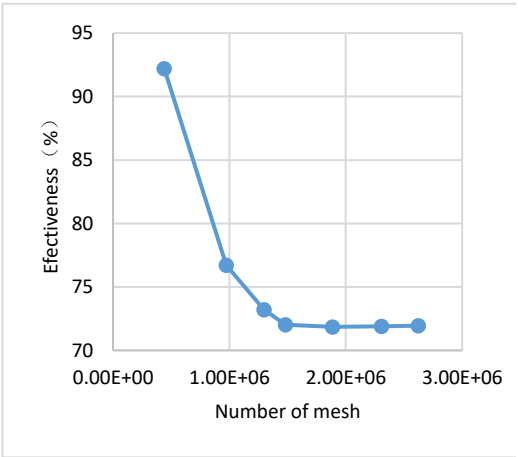

（b）Number of Mesh Elements - Effectiveness Curve

Fig.4 Change of Head and Effectiveness under Different Mesh Elements Number

According to the curves above, it can be observed that when the number of mesh elements is greater than 1298205, the changes of various results tend to be stable. Therefore, the model with the number of mesh elements of 1298205 is selected as the model used for the simulation in this paper.

This paper employed an enhanced wall treatment that created a fine grid near the wall such That y+, which is the non-dimensional distance from the wall to the center of the first grid, was less than 3.

3 Influence of impeller geometric parameters on the performance of the device

In this section, we will use the CFD numerical simulation to identify the influence of geometric parameters of the impeller on the performance of the device to determine the parameters of impeller diameter, blade inlet & outlet angle, length, and the number of blades. By using ANSYS CFX to simulate the impeller with different parameters, the velocity of different planes as well as the changes in head & efficiency were viewed. Among these parameters, the priority was given to the speed-increasing performance of the impeller. When discussing the influence of the impeller geometry parameters on the performance of the anti-wax device, the method of control variables was used. More specifically, when discussing a certain parameter, keep the remaining parameter values unchanged. Correspondingly, when a parameter is determined, the parameter will be used to rebuild and perform the next simulation. When performing simulation in this section, the speed is set to 750 r/min.

3.1 Diameter of impeller

Since the connection between the impeller and the hollow rod is based on threads or couplings, the diameter of the hollow rod must be determined first while developing the diameter of the impeller hub. The purpose of using the hollow rod is to enable the hot washing process. To ensure the minimum hydraulic loss during hot washing, a reasonable hollow rod diameter should be selected. As shown in **Fig. 5**, it is a graph of the total hydraulic loss inside and outside of the hollow sucker rods with different diameters during the well washing. According to the results shown in **Fig. 6**, hollow rods of 34 mm are selected as the rotating shaft of the device, so the diameter of the impeller hub is 34 mm.

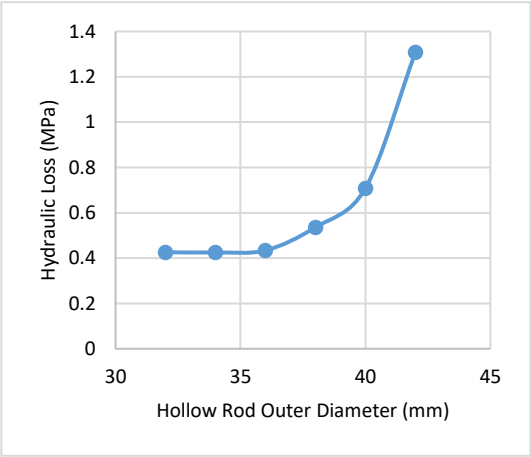

Fig.5 Total Internal and External Hydraulic Losses under Hollow Rods with Different Diameters

Fig. 6 shows the velocity diagrams of the outlet surface obtained after simulating four impellers with different impeller blade diameters.

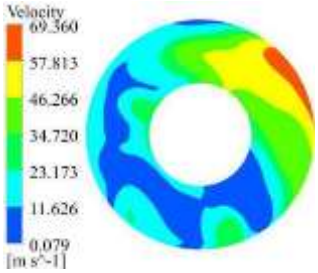

(a) Velocity Diagram of 60 mm Impeller Diameter Outlet Surface

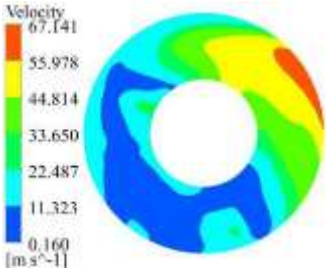

(b) Velocity Diagram of 65 mm Impeller Diameter Outlet Surface

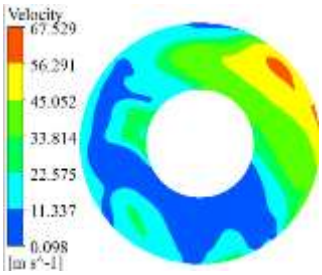

(c) Velocity Diagram of 68 mm Impeller Diameter Outlet Surface

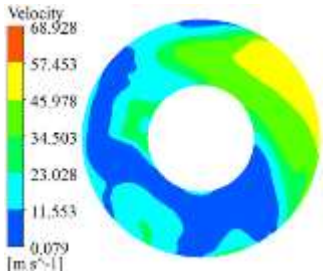

(d) Velocity Diagram of 70 mm Impeller Diameter Outlet Surface

Fig.6 Influence of Impeller blade Diameter on Velocity Diagrams of Impeller Outlet Surface

In these velocity contours, the area of the low-velocity area increased with the upsurge of the diameter. The common feature is that the velocity distribution is not uniform, indicating that the flow of fluid in the watershed is disordered. Thus, the shear stress increased. These changes are beneficial to preventing the formation of wax crystals or destroying the already formed wax crystal structure, to achieve the purpose of preventing wax. **Fig. 7** presented the graphs of the average velocity of the outlet surface of the entire domain, the average velocity of the outlet surface of the impeller domain, and the head and the efficiency as the function of the diameter of the rim.

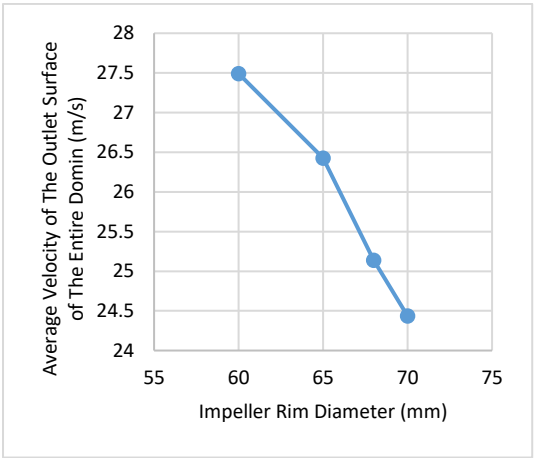

(a) Average Velocity of Outlet Surface of Entire Domain

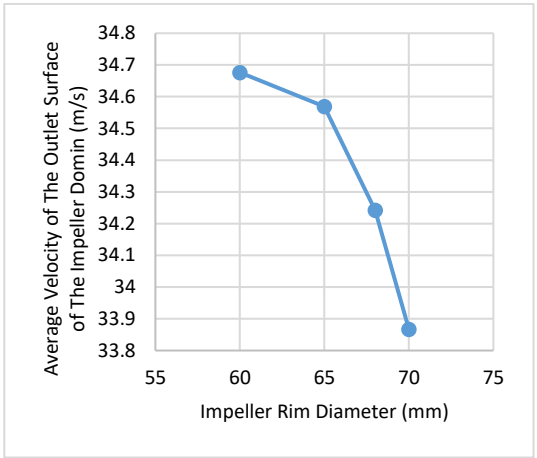

(b) Average Velocity of Outlet Surface of Impeller Domain

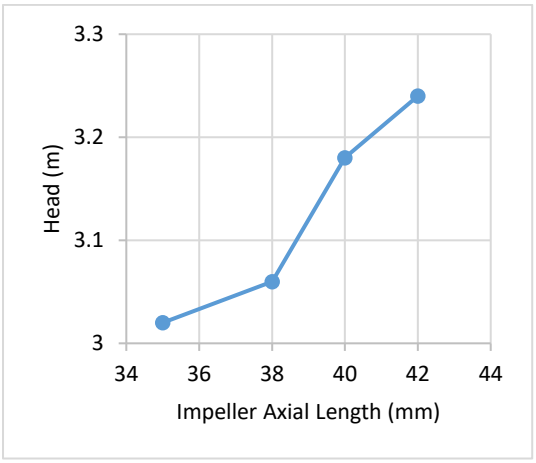

(c) Head

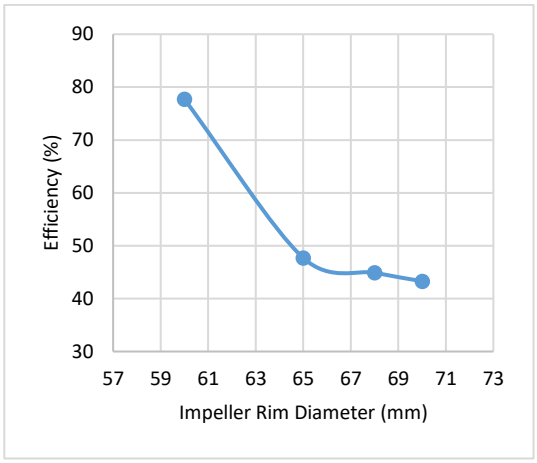

(d) Efficiency

Fig.7 Different Parameters Change with Impeller Rim Diameter

The average velocity of the outlet surface of the entire domain and the outlet surface of the impeller domain decreased with the increase of the diameter of the impeller rim, and a higher flow rate is more conducive to preventing wax deposition. Although the head increased with the growth of the diameter, the efficiency showed a tendency that drops significantly. Taking the above parameters into consideration, the diameter of the impeller rim is determined to be 60 mm.

3.2 Blade inlet and outlet angle

When discussing the influence of the inlet and outlet angle of the blade on the speed-increasing performance of the device, the method used is to perform numerical simulation based on the inlet and outlet angle of the conventional axial flow pump and to check the parameters such as the maximum speed and head of the fluid obtained after the impeller acts. Then according to the simulation results, the dichotomy method is used to increase or decrease the value of the impeller inlet and outlet angles appropriately. In the design of the impeller blade inlet and outlet angle, according to more than 40 sets of impeller cases under different blade inlet and outlet angles, view and compare the speed increase effect to determine the best angle value. **Fig. 8** is a distribution diagram of peak fluid velocity and impeller head obtained after simulating impellers with different angles.

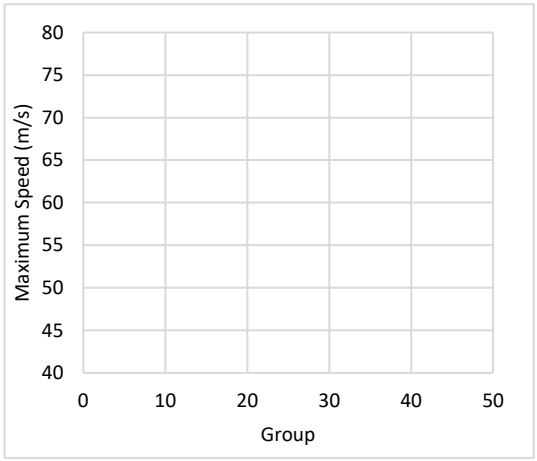

(a) Max Speed Distribution

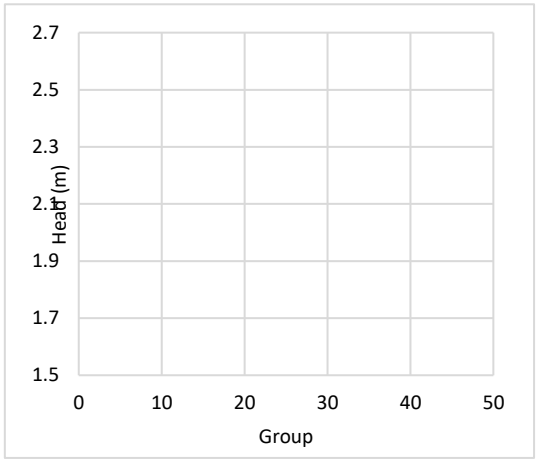

(b) Head Distribution

Fig.8 Head Distribution in Different Sets of Simulation Results

When looking at the effect of different inlet and outlet angles of the impeller on the head, it was found that, in all the simulated cases, the values of the head were distributed between 2.33m and 2.52m. Since the primary consideration is the speed-increasing capability of the impeller, and the head's perception of the blade angle change is not obvious, thus, in this section, the impact of the impeller's inlet and outlet angle is not considered when selecting the impeller blade's inlet and outlet angle. **Table 3** shows the final blade angle values.

Table. 3 Final Blade Inlet and Outlet Angles

β_1	β_2
21.8°	36.5°
18.9°	34.7°
16.4°	33.6°
14.5°	32.8°
12.9°	32.4°

3.3 Impeller axial length

When discussing the impact of the axial length of the impeller on the performance of the device, the length of the impeller must not increase endlessly. Therefore, a reasonable range needs to be set. According to the previously determined impeller parameters, the impeller model is reasonable when the length is within 25 - 42 mm. Otherwise, the values of the blade angles β_1, β_2, and the meridional & tangential blade extension most likely result in abnormal or strange blade shape. In this section, we will conduct a flow simulation for 6 groups of impellers with different lengths in this range, and analyze the changes of the average velocity of the outlet surface of the whole domain, the average velocity of the outlet surface of the impeller domain, head & efficiency with the length of the impeller. **Fig. 9** is the outlet surface velocity diagrams.

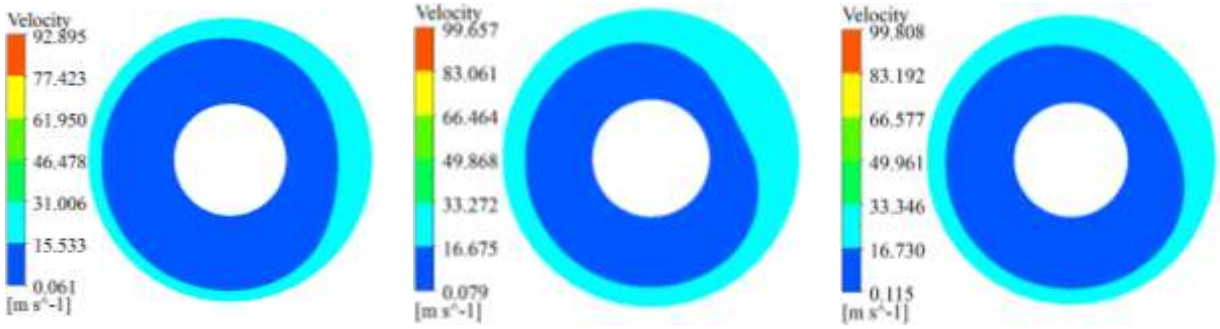

(a) 25 mm length (b) 30 mm length (c) 35 mm length

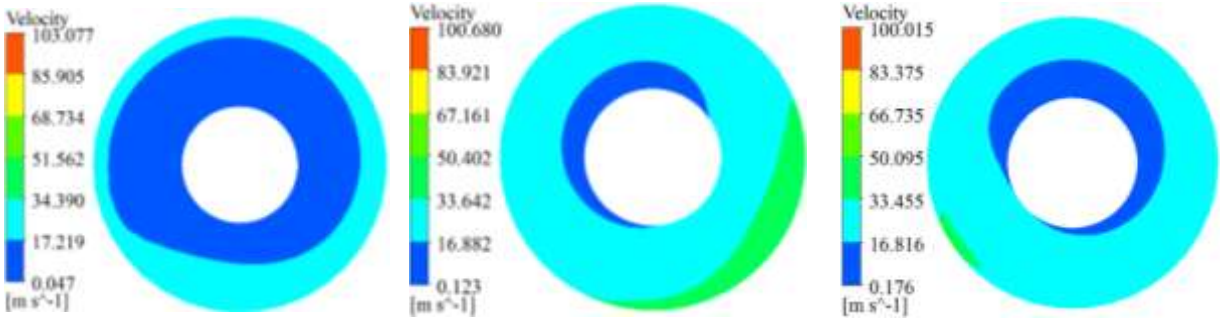

(d) 38 mm length (e) 40 mm length (f) 42 mm length

Fig. 9 The Outlet Surface of the Whole Domain Velocity Diagrams

In **Fig. 9**, the area of the dark blue part represents the low-speed area in the diagrams, which is decreasing with the increase of the impeller length. Under a certain rotation speed, the increase of the blade length makes the impeller fully contact with the well fluid more, and does more work on the fluid. Therefore, the area of the low-speed area is reduced.

Fig. 10 shows the graphs of the average velocity of the impeller domain outlet surface, where head and efficiency were plotted against impeller axial length.

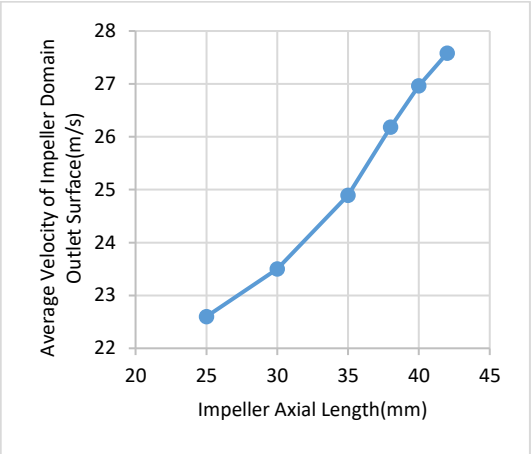

(a) Average Velocity of Impeller Domain Outlet Surface

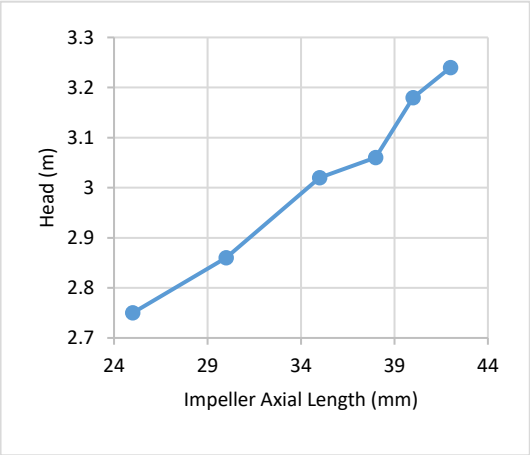

(b) Head

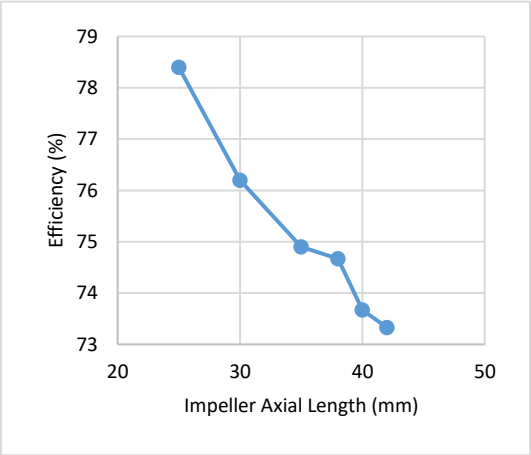

(c) Efficiency

Fig.10 Variation of Various Parameters with The Axial Length of The Impeller

Under the action of the impellers, the average velocity of the impeller domain outlet surface and head increased with the growth of the length of the impeller. The reason is that the greater the axial length of the impellers is, the more complete the conversion of the mechanical energy and fluid kinetic energy of the impellers are. As the well fluid obtains a higher speed, the shear stress in the fluid increased accordingly, which assists prevent wax deposition. Although the efficiency of the impellers has decreased, the axial length increased from 25 to 42 mm. Besides, the head has increased by more than 0.4 m, and efficiency has only decreased by about 5.5%. The results that increased in head and decrease in efficiency is considered to be acceptable, and the impellers with a longer length provided a higher speed-increasing capability. Therefore, the axial length of the impeller is determined to be 42 mm.

3.4 Number of blades

To discuss the influence of the number of blades on the performance of the wax prevention device, this section will simulate the impellers with 4, 5, and 6 blades to determine the optimal number of blades. **Fig.11** shows the velocity diagrams of the outlet surface of the entire domain, the outlet surface of the impeller domain, and the velocity attenuation during the flow of well fluid to the outlet.

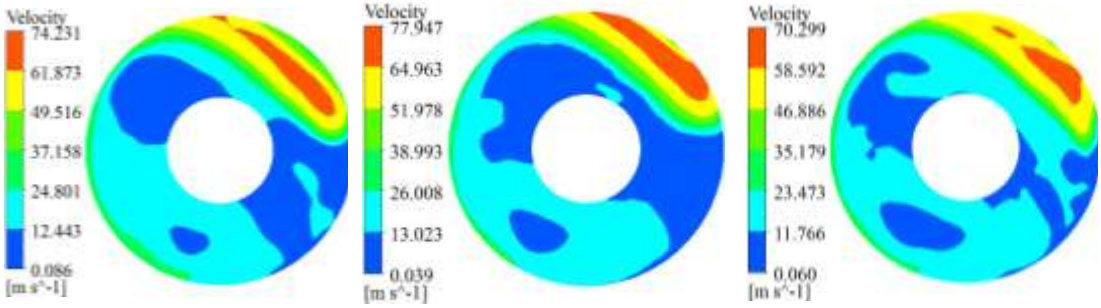

(a) Impeller Domain Outlet Surface of 4-Blades Impeller

(b) Impeller Domain Outlet Surface of 5-Blades Impeller

(c) Impeller Domain Outlet Surface of 6-Blades Impeller

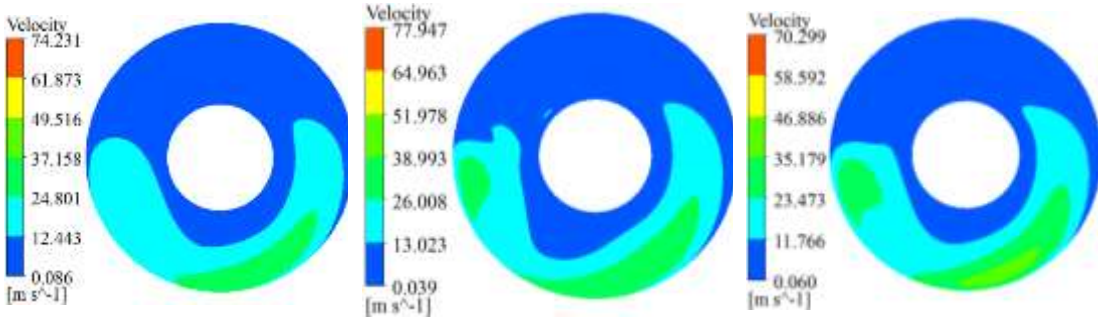

(d) The Entire Domain Outlet Surface of 4-Blades Impeller

(e) The Entire Domain Outlet Surface of 5-Blades Impeller

(f) The Entire Domain Outlet Surface of 6-Blades Impeller

Fig.11 Velocity Diagrams of the Impeller Domain Inlet Surface and the Entire Domain Surface under Different Impeller Numbers

In the above two sets of Velocity Diagrams, it can be observed that, after the fluid passes through the impeller with 5 blades, the maximum velocity obtained by the well fluid is greater. In these velocity diagrams of the outlet surface of the impeller domain, the area of the high-speed area in the velocity diagrams with the number of impeller blades of five is the largest; six is the second, and the number of four is the smallest. After comparing the velocity diagrams of these two groups of different positions, it is found that the high-speed area in the outlet surface of the impeller corresponds to the low-speed position of the outlet surface. The reason for this phenomenon is that there is a spiral flow in the pipeline, and the fluid is undergoing chaotic and disorderly movement. In this case, it is beneficial to prevent the formation of a concentration gradient of wax molecules between the oil and the pipe wall, to achieve the purpose of suppressing wax deposition.

Fig. 12 shows a line chart of the change of the average flow rate of the fluid along the pipeline and the head after the treatments of impellers with different blade numbers. When the well fluid was lifted to the wellhead, the fluid needs to overcome potential energy and viscous losses while the flow rate decreases. As the fluid gradually approaches the impellers, the impellers start to function on the crude oil, where the kinetic energy of the well fluid increases and the flow velocity increases.

Under this effect, the spiral flow will occur in the tubing, and the wax deposition phenomenon can be effectively alleviated. The average speed increases to the peak. After the well fluid gradually disengaged from the impellers, the flowrate began to decrease gradually. In the three sets of data, the impellers with 5 blades have a better speed-increasing effect. Under the treatment of these impellers, the average peak velocity of the fluid obtained is the largest, and, also, the average velocity of the outlet surface of the entire domain is the largest. At the same time, the 5-blade impeller has a larger head.

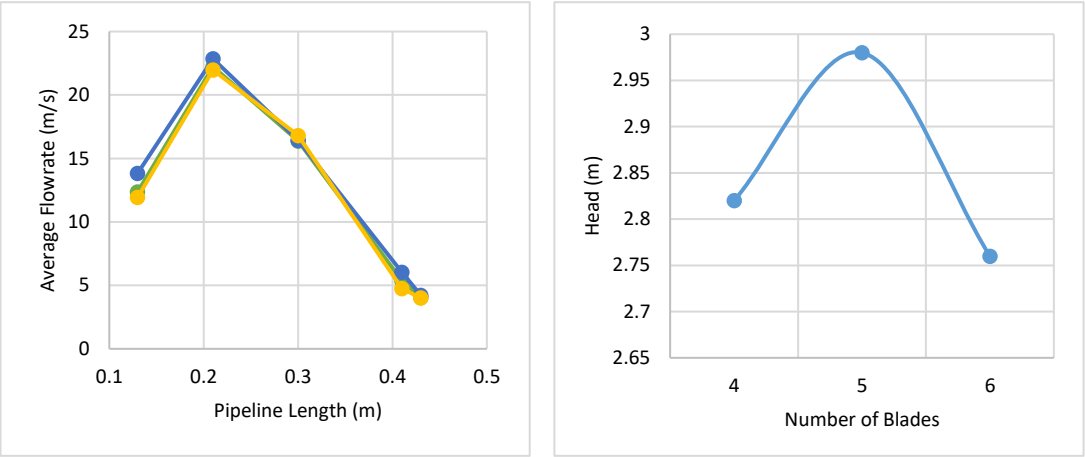

(a) Average Flow rate (b) Head

Fig.12 Changes in Average Flowrate and Head

Under the conditions of the same speed, the changes of different parameters indicated that the 5 blades impeller offered better performance. Although, as the number of blades increases, the effective area through which the fluid can pass becomes smaller, the contact area between the fluid and the impeller increases at the same time as the number of blades increases, and the impellers have a more enough effect on the fluid. Simultaneously, due to the limited space in the tubing, the originally reduced flow area of the impeller will be further reduced under the high-speed rotation of the 6-blade impeller, which will result in greater flow resistance, making the passage of well fluid smaller. Conversely, if the number of blades decreases, the area of the flow channel increases, but the effect of the impellers on the fluid decreases. According to the above results, the 5-blade impellers can produce a more enough effect on the fluid than the 4-blade ones. Compared with the 6-blade impellers, the 5-blade impellers, which has a larger flow channel area, offered better speed-up performance.

4 The influence of equipment technological parameters on performance and application

4.1 Rotational speed of impellers

When the rotational speed of the impellers increases, the well fluid will gain greater kinetic energy, but, in practice, it may not need such a high flowrate. The reason is that, when the velocity is used to prevent wax, the effect will be greatly attenuated as the flow rate increases. Besides, increasing the rotating speed will raise the torque of the rotating shaft, but this will not improve the wax resistance of the device, which will cause a waste of energy. Therefore, a reasonable rotation speed is crucial to the design of the device. In this section, the flow simulation of the impellers under the condition of r=200-1000r/min rotation speed will be carried out, and the rotation speed design of the device will be presented by comprehensively considering the parameters, such as the outlet velocity diagrams and the average outlet velocity changes. **Fig. 13** shows the simulation results.

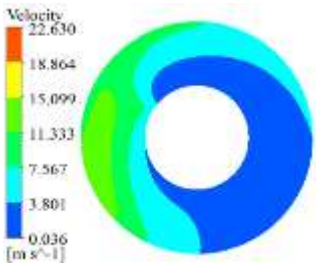

（a）200 r/min-Velocity Diagrams

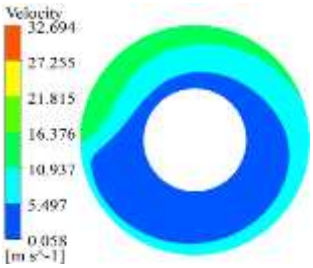

（b）300 r/min-Velocity Diagrams

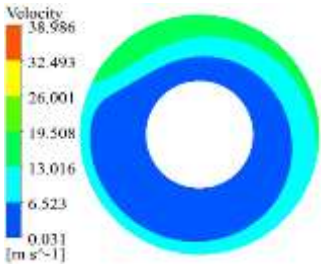

（c）400 r/min-Velocity Diagrams

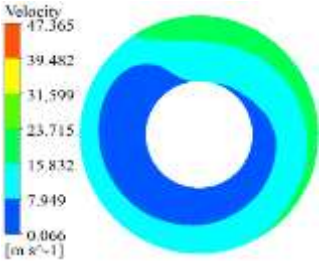

（d）500 r/min-Velocity Diagrams

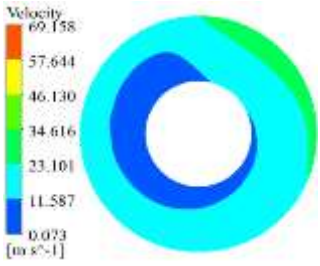

（e）600 r/min-Velocity Diagrams

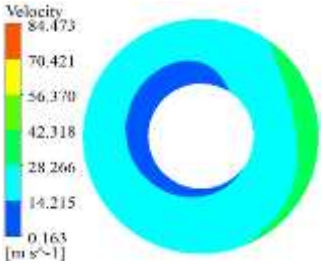

（f）700 r/min-Velocity Diagrams

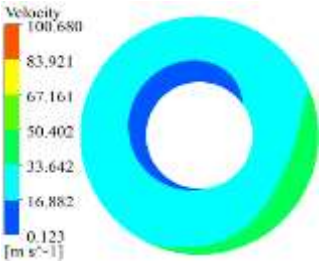

（g）800 r/min-Velocity Diagrams

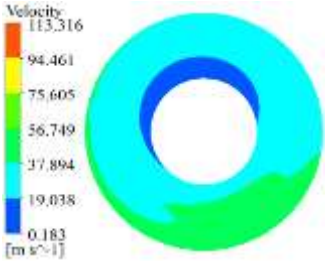

（h）900 r/min-Velocity Diagrams

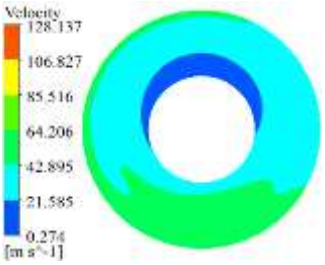

（i）1000 r/min-Velocity Diagrams

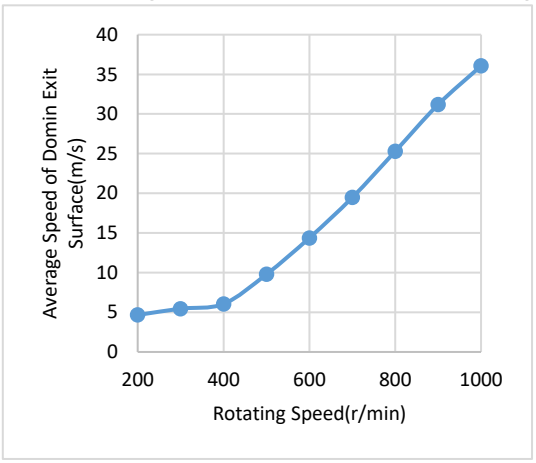

(j)Average Velocity of Outlet Surface

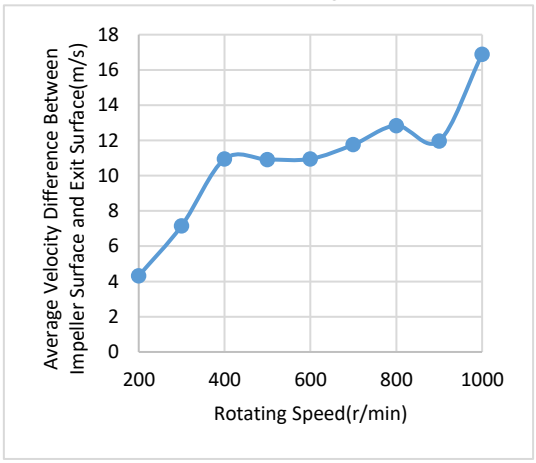

(k) Average Velocity Difference between Impeller Surface and Outlet Surface

Fig.13 Simulation Results under Different Rotation Speeds

The dark blue area in the velocity diagrams is representing the low-speed area. It can be observed that the area will no longer change when the rotation speed reaches 600 r / min. Therefore,

if the rotation speed continues to increase, the effect of increasing the speed on the fluid in the low-speed area will become ineffective. After looking at the change of the average speed of the outlet surface, it is found that when the rotation speed is greater than 400 r/min, the average speed almost increases linearly. Although the average velocity difference between the impeller surface and the outlet surface at 200 r/min is the smallest, this does not prove that the hydraulic loss during the movement of well fluid out of the impeller domain to the outlet surface is the smallest. Considering the anti-wax efficiency of the device, the value of the rotation speed, at which the average flow velocity difference between the outlet surface of the impeller domain and the outlet surface of the entire basin changes smoothly, is selected as the final result. Considering the above factors comprehensively, the value of 600 r/min is finally determined as the rotation speed value of the wax prevention device.

4.2 Impeller position and spacing

Generally, the higher the temperature of the crude oil is, the deeper the oil well is. In this case, even if the flow rate of the well fluid is low, the temperature is still higher than the wax deposition point, where the wax deposition will not occur at this time. Therefore, the impeller of the impeller-type speed-increasing anti-wax device can be placed in a downhole position, where wax is more likely to form. Considering the actual situation of different oil wells, according to the difficulty of waxing in deep wells, the oil pipes are unevenly arranged at intervals with different densities. In this paper, the distance between the two wax-proof devices is called intervals, and the number of a wax-proof device arranged in the wellbore per unit length is called density.

4.3 Device anti-wax application in oilfield well

To verify the wax prevention performance of this impeller diversion wax prevention device in actual production, two submersible screw pump wells with different parameters were tested. **Table 4** shows the relevant parameters of the experimental oil wells.

Table. 4 Related Parameters of Two Experimental Oil Wells

Well ID	Pump Type	Pump Speed	Water Cut	Pump Efficiency	Daily Oil Production	Working Level	Well Length
#1	500-14	120 rpm	87.5%	45.1%	70 t/d	342 m	1000 m
#2	120-27	70 rpm	89.5%	49.7%	15 t/d	813 m	980 m

The experiment was conducted for 30 days. The data was measured every three days, including daily fluid production, the electric current of the pump, and working-level changes. The results were compared with the parameters of the oil well when the device was not used. Before experimenting, the two experimental oil wells were separately hot washed to ensure that no wax was deposited in the well. **Fig. 14** shows some graphs drawn according to the data after conducting experiments on two oil wells.

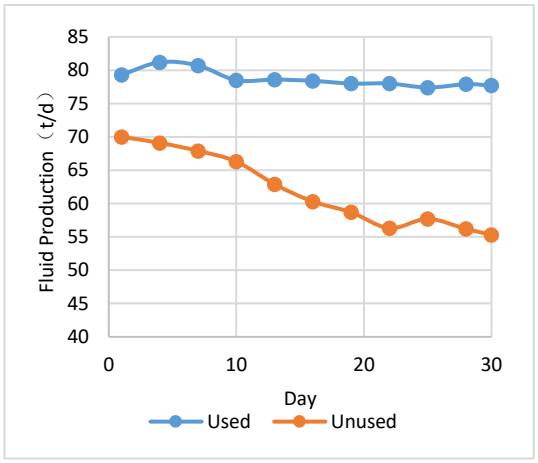

(a) #1 Daily Fluid Production

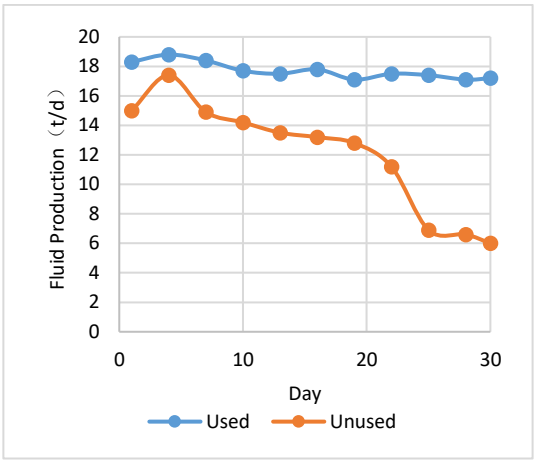

(d) #2 Daily Fluid Production

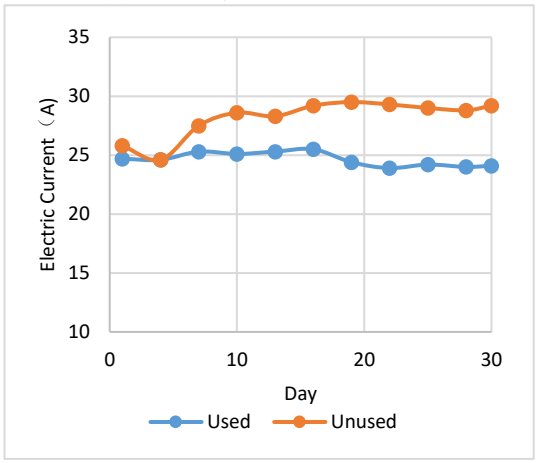

(b) #1 Electric Current of Pump

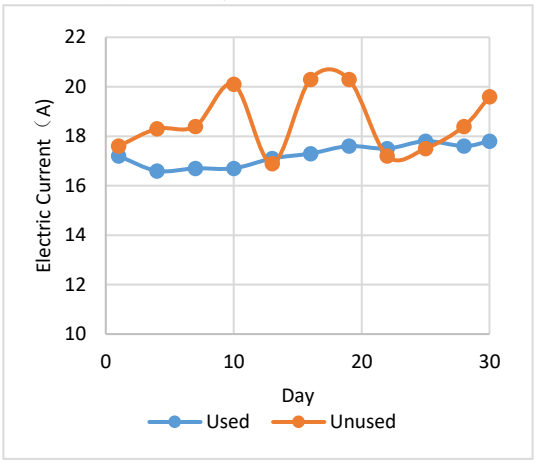

(e) #2 Electric Current of Pump

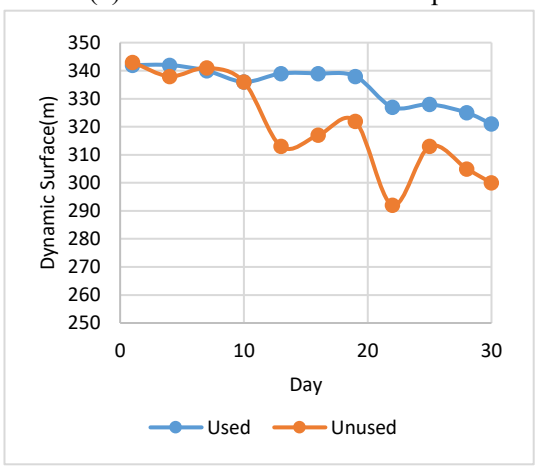

(c) #1 Working Level

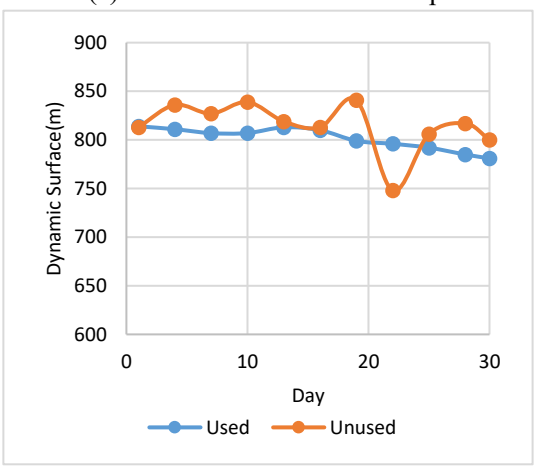

(f) #2 Working Level

Fig. 14 Anti-wax performance test results

According to the results shown in the figure above, both sets of experiments showed the same trend. Compared with the non-used impeller diversion wax prevention device, the daily fluid production changed steadily, and at the same time, the output is improved, indicating that it can increase oil production. Besides, the electric current output decreased, and the electric current after 30 days was not much different from the current at the beginning of the experiment. It indicated that the increase in pump load due to wax deposition was not obvious. Although there is still a downward

trend in the working level, the amplitude is small, and it has been significantly improved after using the device. The changes in the above parameters have proved that the device has a favorable wax-proof function and has the property of increasing oil extraction. When it is used to assist oil recovery, it can effectively prevent the occurrence of wax deposition and ensure the normal operation of oil recovery equipment.

The application of the impeller-type speed-increasing anti-wax device can effectively delay the occurrence of wax deposition, thereby greatly prolonging the well washing cycle. The traditional hot washing process will bring about a series of adverse effects, such as high costs, environmental pollution, and affecting the normal production of oil wells. At the same time, after the application of the device, the production of oil increases due to the growth of the flow rate of crude oil and the reduction in the number of well shutdowns, which can bring considerable economic benefits. Besides, the use of speed-increasing anti-wax technology not only opened up a novel way to clean the wax control technology but also provided researchers with new ideas to deal with the wax deposition in oil wells.

RESULTS

To ensure that the core components of the device, which are the impellers, have better hydraulic performance, CFD was used to study the influence of the impeller structure parameters and device process parameters on the performance of the wax prevention device. The results showed that the increase in the diameter of the impeller rim will cause a decrease in the speed-increasing performance of the impellers. The change of the blade angle will affect the speed-increasing performance of the impellers, but the changes in head and efficiency are not obvious. As the increase in axial length enlarges the work of the impeller on the well fluid, the impellers with a longer length have a higher speed-increasing capability. The impellers with 5 blades can obtain a better balance between the flow area in the pipe and the effect on the fluid, so no matter the external characteristics or speed-increasing performance, the impellers with 5 blades can provide better performance.

Table. 5 Main Structural Parameters of Anti-Wax Device

Hollow Rod Diameter / Impeller Hub Diameter	Impeller Rim Diameter	Impeller Blade Angle		Impeller Axial Length	Number of Impeller Blades	Impeller Blade Thickness	Rotational Speed	Impeller Installation Position	Impeller Spacing
		β_1	β_2						
36mm	60mm	21.8°	36.5°	42mm	5	1mm	600 r/min	Locations where wax is likely to form downhole	3m /Pc
		18.9°	34.7°						
		16.4°	33.6°						
		14.5°	32.8°						
		12.9°	32.4°						

In terms of the influence of the rotation speed on the performance of the device, although the increase of the rotation speed will make the well fluid obtain a greater flow rate, it is unreasonable to increase the rotation speed blindly when considering the anti-wax efficiency of the device. Combined with the change of head under different rotation speeds and the attenuation of fluid flow rate, the rotation speed of the device was determined to be 600 r/min. The impellers are installed in

series in the oil well at the wax-prone position. The specific position needs to be determined by different oil wells, and the spacing is the value of the impeller's head. **Table 5** shows the main structural parameters of the impeller speed-increasing anti-wax device.

Experiments were carried out on the two submersible screw pump oil wells in the Daqing oilfield, using impeller-type speed-increasing and wax-proof devices. The test results showed that the two oil wells, which originally had serious waxing phenomena, has been significantly improved in oil production. Besides, in these two wells, the fluid production increased, the current output decreased, and the overall change was stable, indicating that the wax prevention device has favorable wax prevention performance.

CONCLUSION

According to the relationship between the flow rate of crude oil and wax deposition, an impeller-type speed-increasing wax prevention device is designed. As a physical wax removal device, it can increase the velocity of well fluid, which can prevent the deposition and aggregation of wax molecules during crude oil production.

Based on fluid mechanics, through the simulation of multiple sets of impellers with different structures, it is found that impellers with reasonable parameters can play a significant role in the speed-up performance of the device.

For this type of impeller type speed-increasing anti-wax device, the recommended rotating speed is 600 r/min. If the speed is too low, it will affect the wax prevention performance of the device; on the contrary, it will affect the wax prevention efficiency of the device and cause a waste of energy.

Experimental results showed that this impeller-type speed-increasing wax-proof device has a great wax-proof performance. At the same time, it can meet the wax protection requirements of oil wells with different characteristics, and its application can bring considerable economic benefits. Besides, it is of great significance to the improvement and innovation of anti-wax technology.

ACKNOWLEDGMENTS

The project was funded by Natural Science Foundation of Heilongjiang province (No. LH2019E018), Natural Science Foundation of China (No.51774091; 51607035), Heilongjiang Postdoctoral Research Foundation (LBH-Q20083; LBH-Q18029), EPSRC Doctoral Training Partnership (EP/R513222/1), Daqing guiding science and technology planning project (zd-2019-20). China Postdoctoral Science Foundation (2018M641804).

REFERENCE

[1] Al-Yaari, M. Paraffin wax deposition: Mitigation and removal techniques. SPE Saudi Arabia section Young Professionals Technical Symposium. Society of Petroleum Engineers, 2011, 2-17. https://doi.org/10.2118/155412-MS.

[2] Wei, J. Research on Waxing Eegularity and Wax Removal Technology of Rodless Lifting Oil Wellbore. Chemical Engineering & Equipment, 2019(09): 108-111. https://doi:10.19566/j.cnki.cn35-1285/tq.2019.09.049.

[3] White, M., Pierce, K., Acharya, T. A review of wax-formation/mitigation technologies in the petroleum industry. SPE Production & Operations. 2017,33(3): 476 – 485. https://doi.org/10.2118/189447-PA.

[4] Sousa, A.L., Matos, H.A. Guerreiro, L.P. Preventing and removing wax deposition inside vertical wells: a review. J Petrol Explor Prod Technol 2019,9(3):2091–2107.

https://doi.org/10.1007/s13202-019-0609-x.
[5] Janamatti, A., Lu, Y., Ravichandran, S., Sarica, C., & Daraboina, N. Influence of operating temperatures on long-duration wax deposition in flow lines. Journal of Petroleum Science and Engineering. 2019(2019). DOI:10.1016/j.petrol.2019.106373.
[6] Dong, Z. H., Yang, F. R. Wang, F. etc. Application and Structure of Pollution Prevention Column for Wax Cleared. Oil Field Equipment, 2012(6):78-80. https://doi.org/10.2118/65380-MS.
[7] Li, Y. Research and Application of Cleaning Technology for Cleaning Wax. Chemical Engineering Design Communications. 2017, 43(5):1. https://doi:10.3969/j.issn.1003-6490.2017.05.090.
[8] Dong, L. J., Xie, H. Z., Zhang, F. S. Chemical Control Techniques for the Paraffin and Asphaltene Deposition. SPE International Symposium on Oilfield Chemistry. 2001, 1-11. https://doi.org/10.2118/65380-MS.
[9] Anisuzzaman, S.M., Abang, S., Bono, A., Krishnaiah, D., Ismail, N.M., San-drison, G.B. (2017) An evaluation of solubility of wax and asphal-tene in crude oil for improved flow properties using a copolymer solubilized in organic solvent with an aromatic hydrocarbon. World Academy of Science, Engineering and Technology. 2017, 130(10):688 – 695. https://doi.org/10.5281/zenodo.1132375.
[10] Dobbs, J. B. A Unique Method of Paraffin Control in Production Operations. SPE Rocky Mountain Regional Meeting. 1999, 1-6. https://doi.org/10.2118/55647-MS.
[11] Khaibullina, K. Technology to Remove Asphaltene, Resin and Paraffin Deposits in Wells Using Organic Solvents. SPE Technical Conference and Exhibition. 2016, 32-44. https://doi.org/10.2118/184502-STU.
[12] Santamaria, M. M., George, R. E. Controlling Paraffin-Deposition-Related Problems by the Use of Bacteria Treatments. SPE Annual Technical Conference and Exhibition, 6-9 October, 2019, Dallas, Texas. 1991: 351-361. https://doi.org/10.2118/22851-MS.
[13] Jessen, F. W., Howell, J. N. Effect of flow rate on paraffin accumulation in plastic, steel, and coated pipe. Petroleum Transactions of the AIME, 1958, 213(4):80-84. https://doi.org/10.2118/968-G.
[14] Hartley, R., Jadid, M. B. Use of Laboratory and Field Testing to Identify Potential Production Problems in the Troll Field. SPE Production Engineering, 1989, 4(1):34-40. https://doi.org/10.2118/15892-PA.
[15] Hsu, J. J. C., Santamaria, M. M., Brubaker, J. P. Wax Deposition of Waxy Live Crudes Under Turbulent Flow Conditions. SPE Annual Technical Conference and Exhibition, 25-28 September, New Orleans, Louisiana. 1996: 179-192. https://doi.org/10.2118/28480-MS.
[16] Nazar, A. R. S., Dabir, B., Vaziri, H., Islam, M. R. Experimental and Mathematical Modeling of Wax Deposition and Propagation in Pipes Transporting Crude Oil. SPE Production and Operations Symposium, 24-27 March, Oklahoma City, Oklahoma, 2001, 27(1-2):185-207. https://doi.org/10.2118/67328-MS.
[17] Mirazizi, H. K., Shang, W., Sarica, C. Experimental investigation of paraffin deposition under turbulent flow conditions. 8th North American Conference on Multiphase Technology, 20-22 June, Banff, Alberta, Canada, 2012: 61-73. https://www.onepetro.org/download/conference-paper/BHR-2012-A010?id=conference-paper%2FBHR-2012-A010.
[18] Rittirong, A., Panacharoensawad, E., Sarica, C. Paraffin deposition under two-phase gas-oil slug flow in horizontal pipes. SPE Production & Operation, 2017(01): 99-117.

https://doi.org/10.4043/26047-MS.
[19] Theyab, M. A., Diaz, P. A. Experimental Study on the Effect of Spiral Flow on Wax Deposition Volume. Abu Dhabi International Petroleum Exhibition & Conference, 7-10 November, Abu Dhabi, UAE. 2016, 172-190. https://doi.org/10.2118/182936-MS.
[20] Albagli, R. C., L. B. Souza, A. O. Nieckele. Reynolds Number Influence on Wax Deposition. OTC Brasil, 24-26 October, Rio de Janeiro, Brazil. 2017: 41-50. https://doi.org/10.4043/28053-MS.
[21] Alnaimat, F., Ziauddin, M. Wax deposition and prediction in petroleum pipelines. Journal of Petroleum Science and Engineering. 2020, (2020). https://doi.org/10.1016/j.petrol.2019.106385.
[22] Versteeg, H. K., Malalasekera, W. An introduction to Computational Fluid Dynamics: The Finite Volume Method. Pearson Schweiz Ag, 2007, 20(5):400.